

Beyond the \sqrt{N} -limit of the least squares resolution and the lucky model

Gregorio Landi^{a*}, Giovanni E. Landi^b

^a Dipartimento di Fisica e Astronomia, Universita' di Firenze and INFN
Largo E. Fermi 2 (Arcetri) 50125, Firenze, Italy

^b ArchonVR S.a.g.l.,
Via Cisieri 3, 6900 Lugano, Switzerland.

April 29, 2019

Abstract

A very simple Gaussian model is used to illustrate a new fitting result: a linear growth of the resolution with the number N of detecting layers. This rule is well beyond the well-known rule proportional to \sqrt{N} for the resolution of the usual fit. The effect is obtained with the appropriate form of the variance for each hit (measurement). The model reconstructs straight tracks with N parallel detecting layers, the track direction is the selected parameter to test the resolution. The results of the Gaussian model are compared with realistic simulations of silicon microstrip detectors. These realistic simulations suggest an easy method to select the essential weights for the fit: the lucky model. Preliminary results of the lucky model show an excellent reproduction of the linear growth of the resolution, very similar to that given by realistic simulations.

Keywords: Least squares method, Resolution, Position Reconstruction, Center of Gravity, Silicon Micro-strip Detectors, Lucky Model.

PACS: 07.05.Kf, 06.30.Bp, 42.30.Sy

Contents

1	Introduction	2
2	A simple Gaussian model and the linear growth	3
3	The schematic model	5
4	The lucky model	6
4.1	The linear growth in the lucky model	8
5	Hints for an experimental verification	9
6	Conclusions	9

*Corresponding author. Gregorio.Landi@fi.infn.it

1 Introduction

An essential source of information in high energy physics experiments is the tracking of ionizing particles. To accurately collect this information, large arrays of particle detectors (trackers) are installed in the experiments. Among the types of particle detectors, silicon microstrip detectors are frequently selected as tracker components. A silicon microstrip detector has a very special surface treatment (strips) able to give a set of localized signals (hit) to the readout system if a ionizing particle crosses the detector. The algorithms for track reconstruction are essential completions of the tracking systems and large efforts are dedicated to optimize their efficiency. Our refs. [1, 2] were dedicated to these improvements. There we introduced very special probability distributions, one for each hit, calculated for minimum ionizing particles (MIPs) crossing a microstrip detector. These probability distributions are constructed around the form of the hit positioning algorithms. For the hit positioning algorithm we used the center of gravity (COG), the easiest and most frequently employed algorithm ($x_{gj} = \sum_{i=1}^j E_i \tau_i / \sum_{i=1}^j E_i$, where E_i is the signal of the strip i , τ_i its position and j the number of accounted strips). Even if the COG is often indicated as a single algorithm, it has different forms and properties depending by the number j of strip signals inserted in the algorithm. Each COG form has very different analytical and statistical properties and the mixture of different forms must be accurately avoided. In the present developments, the two or three strip COG (COG₂ or COG₃) are the only used forms. Their general expressions contain ratios of random variables that introduce Cauchy-like tails in their probability distributions. Equation 3 of ref. [2] illustrates this property for the COG₂ algorithm. The long equations for the COG_j probability distribution, extended form of eq.5 of ref. [2], are only a part of our needs, to be useful in a fit, they must be completed with the functional dependence from the MIP impact point. This dependence is inserted with the functions of eq.3.2 of ref. [1], they were extracted from the data of a test beam with the use of a theorem demonstrated in section 3.2 of ref. [1]. These functions are expressed with a Fourier series with many terms (150-200). The essential deviation of our complete probability distributions from Gaussian forms obliges the use of maximum likelihood method. With such complex functions, the maximum-likelihood method requires many cares to avoid the non-convergence of the search at the absolute maximum. To improve the convergence we developed a lower level fitting tool (called schematic model) to be used as initialization of the likelihood exploration. The schematic model was built around effective variances extracted from our complete probability distributions, cutting their Cauchy-like tails to avoid divergences (eq.11 ref. [2]). The η -algorithm gives the reconstructed hit positions (eq.8 of ref. [2]). The definition of an effective variance (weight) for each hit allows to determine the initial parameters of the likelihood exploration with a weighted least squares. The first application of our complete method was the reconstructions of straight tracks (ref. [1]), in this case the likelihood is a surface and the convergence to the maximum can be easily followed. The results of the fits showed drastic improvements of the reconstructed track parameters compared to standard fits. The complete method is able to obtain excellent fits even in presence of large outlayers, hence our method eliminates the outlayers from list of fitting problems. For its simplified form, the schematic model is unable to handle the outlayers, but it is very realistic in all the other aspects. After acquiring confidence with straight tracks, we tested the reconstruction of tracks of MIPs in a homogeneous magnetic field (ref. [2]). Even the momentum reconstruction turns out much better than that of the standard fit. In fig. 8 of ref. [2] we reported an interesting effect: an approximate linear growth of the momentum resolution with the number N of detecting layers. This result is strikingly different from the textbook result that easily demonstrates a growth in resolution as \sqrt{N} in least squares. Even if \sqrt{N} refers to the fit of a constant, we will recall this type of rule even for other fitted parameters where the rule is not so simple. The aim of this work is the illustration of the generality of the linear growth in resolution. For this, we study the fit of the track direction of a MIP crossing a simpler tracker at orthogonal incidence. The tracker model is formed by N detecting layers of identical technology, without magnetic field and exposed to a set of parallel tracks of high momentum MIPs (to neglect the multiple scattering). To fix the ideas we suppose silicon micro-strip detecting layers, but, this one is not an essential condition. The simplicity

of the simulations gives a direct explanation of the results of our complete fitting method. Let us briefly recall the principal assumptions contained in the standard least squares method. Very often, identical variance for all measurements is assumed [3]. The identity of the variances is defined in statistics as homoscedasticity. It introduces a drastic shortcut in the least squares equations that become independent from the data variances. The opposite of homoscedasticity is indicated as heteroscedasticity. In this case the identity of the variances is abandoned. The equations for the least squares report the weighted form (as in ref. [4]), but, without additional mathematical tools (as those we developed) it is impossible to consistently handle all the forms of heteroscedasticity. In any case, it is evident that the complexity introduced by heteroscedasticity must be finalized to a gain of resolution. To illustrate this point beyond the results of refs. [1, 2] and their long maximum likelihood searches, a simple Gaussian model will be tested. The model easily shows the generation of the linear growth with N of the resolution even with a very simple form of heteroscedasticity. This Gaussian model is compared with a more realistic model (the schematic model of refs. [1, 2]). We limit the schematic model to a single detector type, very similar to silicon strip detectors largely used in running CERN-LHC experiments [5, 6, 7]. A preliminary introduction of a fast suboptimal tool (the lucky model) will be discussed and compared with the schematic model. We limit our discussion to the recipes to obtain these results. Mathematical details will be published elsewhere.

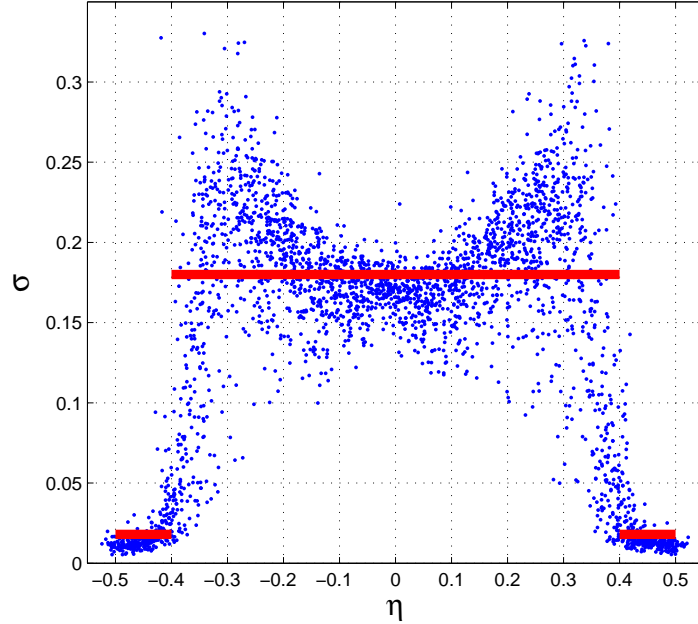


Figure 1: The red lines are the values of σ for the Gaussian model. The blue dots are the effective σ of the schematic model. The dimensions are in strip width ($63\mu m$). The η -algorithm gives the hit positions, with zero as the strip center.

2 A simple Gaussian model and the linear growth

The model we explore is a Gaussian model with two different standard deviations (σ), one of 0.18 (in unity of the strip width $63\mu m$) with a probability of 80 % and the other of 0.018 with a probability of 20%: hard symmetry with a small "spontaneous" symmetry breaking. The relation of this model with the schematic model of silicon micro-strips is illustrated in fig. 1. It represents a drastic simplification of the models of refs. [1, 2]. Experimental hints of the border effect, evident in fig. 1 as a strong decrease

of the effective σ , are reported in ref. [8] for gas ionization chambers.

Few lines of MATLAB [9] code suffice to produce this simulation, and they could be a viable substitute of long mathematical developments. A large number of Gaussian random numbers, with zero average and unity standard deviation, are generated (with the MATLAB `randn` function). Each one is multiplied by one of the two standard deviations (0.18, 0.018) with the given relative probability (80%, 20%). The data are scrambled and recollected to simulate a set of parallel tracks crossing few detector layers. This data collection simulates a set of tracks populating a large portion of the tracker system with slightly non-parallel strips on different layers (as it always is in real detectors). The detector layers are supposed parallel, but for the non-parallelism of the strips, the hit positions of a track, relative to the strip centers, seem to be uncorrelated. The properties of the binomial distribution produce the linear growth. Due to the translation invariance, the tracks can be expressed by a single equation $x_i = \beta + \gamma y_i$ with $\beta = 0$ and $\gamma = 0$ for the orthogonal incidence of the set of tracks (β is the impact point of the track, γ the direction, y_i the positions of the detector layers and x_i the hit position). The distributions of γ_f , the γ value given by the fit, are the object of our study. The γ distribution is a Dirac δ -function, as it is usual to test the resolution of the fitted values γ_f . The distance of first and the last detector layer is the length of the PAMELA [14] tracker (445 mm, 7063.5 in strip width), but this is not essential. Other "detector layers" are inserted symmetrically in this length. Two different least squares fits are compared. One uses identical σ of each hit (we call this standard fit). The other fit applies the appropriate σ -values to each hit. This second fit shows a linear growth in the resolution (as far as a set of random variables can follow this rule). We generate 150,000 tracks for each configuration.

The results are reported in fig. 2 as (empirical) probability density functions of γ_f . The parameter γ_f is the tangent of a small angle, a pure small number. To give a scale to the plots of γ_f , we could identify the tangent with its argument and consider the horizontal scale in radians (rad) and the vertical scale as rad^{-1} . We will neglect all these details in the plots that report probability density functions of pure number variables.

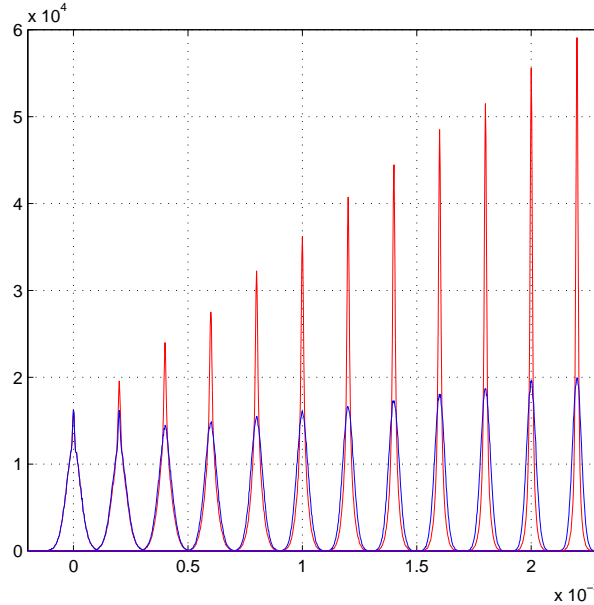


Figure 2: *The Gaussian model. The blue lines are the γ_f -distributions of the standard fit. The red lines are the γ_f -distributions of the σ -weighted least squares, they show a linear growth in the resolution. The first distribution is centered on zero, the others are shifted by $N-2$ identical steps.*

All the distributions we have to plot are centered around their fiducial value $\gamma = 0$ for each number N

of layers. For clarity of the plot, the distributions with two layers is centered on zero. The others with three, four, etc. up to thirteen layers are shifted by $N - 2$ identical steps to show better their increase. (This rule is extended to all similar plots.) Heteroscedasticity influences the first two distributions (two and three layers) even in the standard fit. In fact, if the two hits of a track have a narrow (Gaussian) position distributions (small σ), the γ_f of the fitted tracks is forced to be contained in a narrow distribution. It is curious that to reach the height of these two distributions the standard fits require many additional layers. We will consider the height of each distribution as an evaluation of the resolution of the corresponding fit. Actually, the most common distributions have the maximum proportional to the inverse of the full-width-at-half-maximum (FWHM). The FWHM is often considered a measure of the mean error for non-Gaussian distributions and its inverse is the resolution. If the detector layers are slightly different (as usual) the linear growth will show small distortions due to these differences.

An approximate linear growth can be extracted even from the standard least squares, as illustrated in fig. 3.

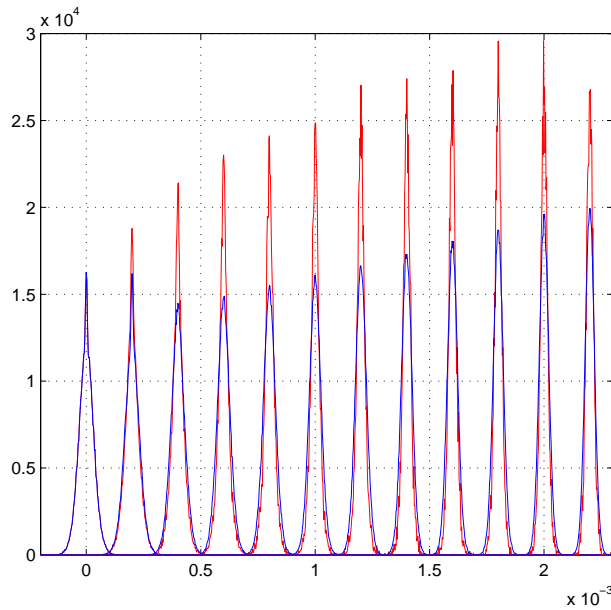


Figure 3: *The Gaussian model. Extraction of an approximate linear growth from the standard least squares with the selection of low ψ^2 -values.*

In fact, for a pure homoscedastic Gaussian model, it is a basic demonstration [3] that the fitted parameters are independent random variables (easily verified in these simulations using a single average σ). The presence of a small heteroscedasticity destroys this independence and tends to couple the probability distribution of γ_f with the values of $\psi^2 = \sum_i (x_i - \beta_f - \gamma_f y_i)^2$ for each track. The parameters β_f and γ_f are those given by the fit of that track. Among the lowest values of the ψ^2 , good γ_f -values are more frequent to find. The Gaussian model shows a partial linear increase of the γ distributions selected with ψ^2 . We used the following empirical equation $\psi^2 < 0.08(N/13)^2$ to account for the ψ^2 increase with N . Figure 3 shows the result of the selection, this violation can be an independent test of heteroscedasticity.

3 The schematic model

Similar results can be obtained from our schematic model. This realistic model is called schematic in refs. [1, 2]. There it was used a first approximation of the complete model and as the starting point for the maximum likelihood search. The quality of the fit produced by the schematic model is not far from

the complete model, the main differences are in the ability of the complete model to find good results even in presence of the worst hits (*outliers*). The calculations of the effective variance of each hit is very time consuming, but after an initial (large) set of σ is obtained, the others can be quickly produced with interpolations (high precisions are inessential). We always used the time consuming procedure. Figure 1 shows a subset of effective σ for this type of micro-strip detectors. An interesting aspect of this scatter-plot is the very low values of σ at the strip borders. The positioning algorithm is the η -algorithm of ref. [10], briefly summarized at pag.8 of ref. [2]. This algorithm is essential to eliminate the large systematic errors of the two strip center of gravity (COG₂). The forms of those systematic errors were analytically described in ref. [11], many years later than their full corrections. References [12, 13] added further refinements to the η -algorithm and extended it to any type of center of gravity (COG) algorithm.

We underline that the results, shown in the following, are impossible without the η -algorithm. For example, the COG₂ algorithm degrades its (modest) results with this refined approach. It is uncertain that the statistics has any relation with least squares fits based on COG positioning algorithms. We proved in ref. [2] that the elimination of any random noise (the statistics) does not modify the probability distributions of the fit products based on the COG₂ positions. Instead, the distributions of the fit results based on the η -algorithm rapidly converge toward Dirac- δ functions, as it must be.

Again, our aim will be the fit of straight tracks of equation $x_i = \beta + \gamma y_i$ with $\beta = 0$ and $\gamma = 0$ incident orthogonally to a set of detector layers. The properties of the simulated hits are modeled as far as possible on test-beam data [14], as discussed in ref. [1]. Even now, we compare the γ_f distributions given by two types of least squares. One fit uses the different σ (the blue dots) of the scatter plot of fig. 1 for the hit, and the standard least squares that assumes identical variances for the hits. Figure 4 shows these results.

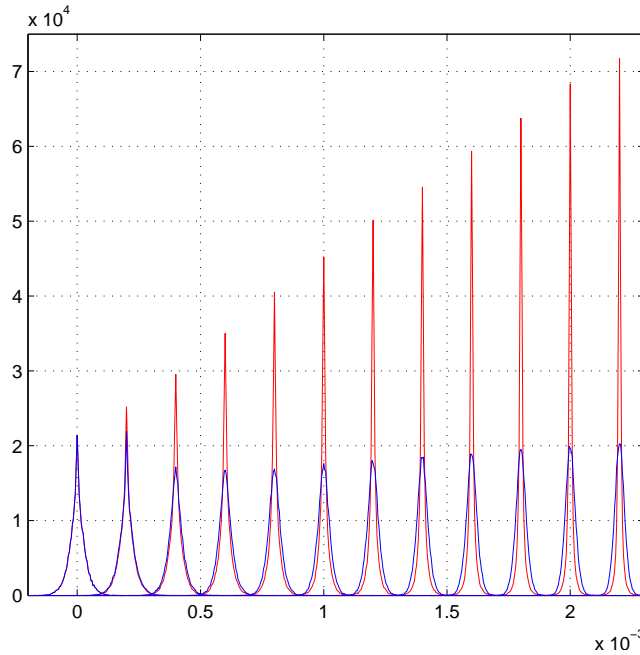


Figure 4: *Schematic model. The blue γ_f distributions are the standard least squares fits. The red γ_f distributions show the linear growth and are produced with the effective σ for each hit*

4 The lucky model

In figure 1 of ref. [2], a large asymmetry is evident in one of the two scatter plots. Given our selection

of an orthogonal incidence, symmetry is expected, but our long list of equations, required to arrive to the effective variances, produce this asymmetry. The sole tentative explanation was the strong similarity of our scatter plots with the COG_2 histograms of the original data. One of the two histograms has the corresponding asymmetry [1]. The data were collected in the test beam of ref. [14]. Our preliminary analysis did not find any simple relation (scaling factors) able to reproduce the plots. The cut selection, we used in the definition of the effective variances (eq.11 of ref. [2]), were essentially based on an aesthetical criterion. We considered relevant the reproduction of parts of the Gaussian features when they were present. Essentially we tuned the cuts on a small subset of excellent hits to seek a comparison with our complete probability distributions. The scatter plots of ref. [1] were produced for the first time just for their insertion in the publication. However, once we discarded the possibility of a casual matching, a reasonable explanation could be found of this coincidence. Thus, a more accurate analysis was undertaken. The use of the equations of ref. [2] allow the construction a very approximate demonstration of the consistency of the trends of our scatter plots. A by-product of that is a geometrical support to the resolution increase at the strip borders, just the origin of the linear growth. All the details of this preliminary demonstration will be published elsewhere, with the hope to obtain something better. For example, simple functions that take into account signal-to-noise ration of each hit. Figure 5 illustrates this very rough matching of the σ scatter plot and the COG_2 histogram. The σ -values are scaled to produce an approximate overlap with the COG_2 histogram. More precisely, we plot the normalized histogram divided by the bin size and interpolated with a Fourier series, the red line is a merged set of dots produced by the interpolation. One red dot for each blue dot.

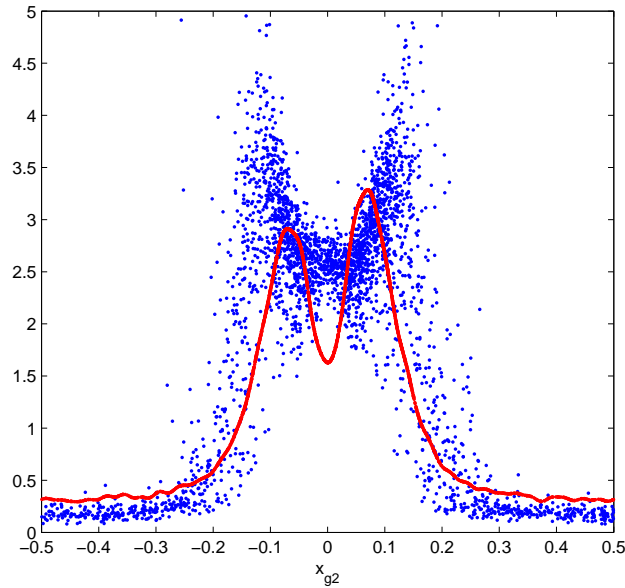


Figure 5: Scatter plot of the effective σ as function of the COG_2 (x_{g2}) scaled to reach an approximate overlap with the COG_2 histogram. More precisely a merged set of red dots corresponding to the blue dots. They are obtained as by-product of the η -algorithm

Here we recall the intuitive explanation given in ref. [1] about this similarity. The effective σ estimates the ranges of the possible impact values converging to the same COG_2 value. Hence, larger σ gives higher COG_2 probability and lower σ gives lower COG_2 probability. Inverting this statement, it looks reasonable that hits with the lower COG_2 probability have lower effective σ and hits in the higher COG_2 probability have higher effective σ . If these assumptions would be successful we have a very economic strategy to implement heteroscedasticity in the track fitting with pieces of information that were well hidden just in front of us. But, without the hints of the scatter plots of ref. [1], they could remain hidden.

The COG_2 probabilities are very easy to obtain from the corresponding histograms or as a by-product of the η -algorithm [12]. Further details are required: the scaling factors to render compatible the COG_2 histograms and effective σ scatter plots. In general, these scaling factors must be calculated. But, for identical detectors, as in our case, an identical factor is required and it becomes irrelevant for the linearity of the (weighted) least squares equations. Hence we can attempt to directly use the amplitude of histogram as rough effective σ and observe the effects in the fit.

4.1 The linear growth in the lucky model

The "lucky" results are illustrated in fig. 6 for this "lucky" model. This figure is produced as fig. 4 with the sole difference given by the use of the rough effective σ in the weighted least squares.

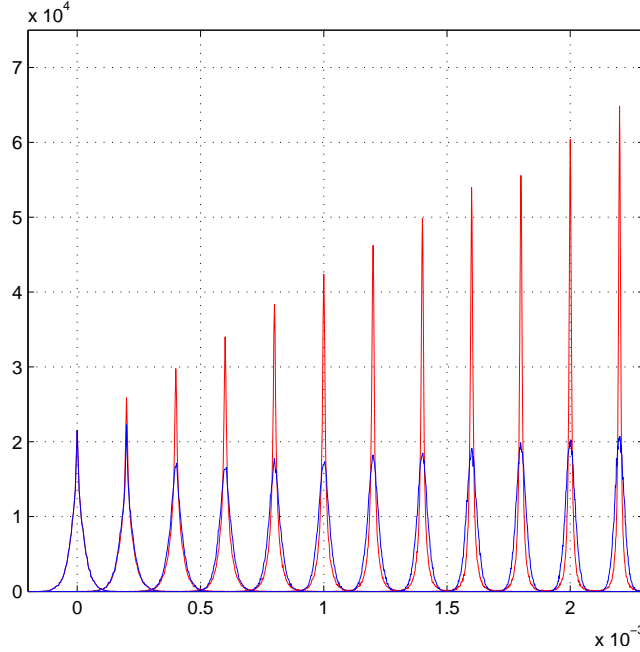


Figure 6: *The lucky model. The blue distributions are the standard least squares. The red distributions are the γ_f given by the lucky model, very near to those of the schematic model.*

The maximum of fig. 6 is around $6.5 \cdot 10^4$ and fig. 4 is around $7.2 \cdot 10^4$ (a difference of 10%): the results of the fits are excellent. The robustness of the heteroscedasticity is evident. Large variations of the details of the parameters (probability distributions) of the models do not modify the fit results. For example, the use of the effective variances, illustrated with the red line in fig. 1, with the η -positioning gives γ_f -distributions identical to the complete schematic model. This result is easy to justify, the weights inserted in the least squares are σ^{-2} , and the higher σ -values are all compressed near to zero, and their differences, compared to the constant value of fig. 1, become negligible. Instead, the lower σ -values are very similar in the two models and they dominate the fits, exactly as for the lucky model. Another connection is contained in the lucky model; the functional form of σ^{-1} as a function of η is well-known function introduced with a theorem in ref. [11] and illustrated in ref. [12]. This function is the average shape of the MIP signal collected by the strip, hence higher signal density gives better hits.

We even test the lucky model approximation with the three strip COG (COG_3) histogram and its corresponding η positioning (η_3). Even here, the linear growth is clearly evident but the maximum is around 1/2 of that of fig. 4. The strip added to the COG_2 , to compose the COG_3 , is almost always pure noise at this orthogonal incidence [12]. In addition, the COG_3 has discontinuities at the strip borders [11],

here very small and masked by the noise, but just in the region with the best σ . Thus this lower result is not unexpected, and it is consistent with our full three strips schematic model. Similar tests were performed on the low noise floating strip side.

5 Hints for an experimental verification

Some of the results presented here could be verified with a test beam. The beam divergence should be less than 10^{-5} radians, probably not easy to obtain. In the simulations we used a very simplified (for the computer) approach: the detector-layer configurations were generated each time dividing symmetrically the allowed interval from the first and last layer. This corresponds to a different experimental set-up for any layer number. A more realistic set-up could be composed with a fixed number of parallel detector layers, (normal silicon micro-strips) orthogonal to the beam (of high momentum to limit the multiple scattering). An effective increase of the layer number can be produced varying those inserted in the fit. Excellent precision in the tracker alignment parameters and a very small beam divergence are required for a direct test of the linear growth. The η -algorithm is essential. At orthogonal incidence and without magnetic field the η -corrections are very small or negligible. In any case for parallel tracks the corrections are identical and their neglect implies a parallel translation of the tracks. The ψ^2 and the lucky model can be used to test heteroscedasticity.

If the beam divergence is large compared to the γ_f -resolution of the fit, the presence of the linear growth in resolution can be observed in the fluctuation of the difference of the γ_f fitted with all the available layers and the γ_f fitted with the elimination of a layer each time in the same track. The linear growth produces a parabolic increase of these differences. Instead, the standard fit produces a small increase in the last couple of differences.

6 Conclusions

Simple simulations produce linear growths in the fit resolution with the number N of detector layers, similar to those of ref. [2] for the momentum reconstruction. Here, sets of parallel straight tracks are used in the fits, and the test parameter is the direction γ of the tracks. This two-parameter fit is easier than that for the momentum. The Gaussian model easily produces the linear growth of the fit resolution. The model is so simple, for its essential mathematics, that it can be completed with few lines of MATLAB code and its results are almost identical to our very complicated schematic model. The addition of the physics of the detectors is a heavy task. The evident similarity of the effective σ scatter-plots with the histograms of the two strips center of gravity triggered a more accurate analysis of its origin. This analysis was sufficiently convincing to try a weighted least squares fit with weights extracted from the center of gravity histogram (the lucky model). The result of this test is excellent with a drastic increase of the fit resolution and the sought linear growth. The differences of the lucky model compared to the schematic model are around 10%, a negligible price compared to the enormous simplification in the extraction of the weights. It is evident that these are very preliminary results, and further tests are essential before a systematic use of the model. Very synthetic indications are given for a experimental verification of the model.

References

- [1] Landi G.; Landi G. E. Improvement of track reconstruction with well tuned probability distributions *JINST* 9 2014 P10006. [arXiv:1404.1968\[physics.ins-det\]](https://arxiv.org/abs/1404.1968)
<https://arxiv.org/abs/1404.1968>

- [2] Landi, G.; Landi G. E. Optimizing momentum resolution with a new fitting method for silicon-strip detectors *INSTRUMENTS* **2018**, 2, 22 arXiv:1806.07874[physics.ins-det] <https://arxiv.org/abs/1806.07874>
- [3] G. Ivchenko and Yu. Medvedev *MATHEMATICAL STATISTICS*-Moscow-URSS-1990
- [4] Olive, K.A.; Agashe, K.; Amsler, C.; Antonelli, M.; Arguin, J.-F.; Asner, D.M.; Baer, H.; Band, H.R.; Barnett, R.M.; Basaglia, T.; et al. Particle Data Group. *Chin. Phys. C* **2014**, 38, 090001.
- [5] ALICE Collaboration. The ALICE experiment at the CERN LHC. *JINST* **2008**, 3, S08002, doi:10.1088/1748-0221/3/08/S08002.
- [6] ATLAS Collaboration. The ATLAS experiment at the CERN Large Hadron Collider. *JINST* **2008**, 3, S08003, doi:10.1088/1748-0221/3/08/S08003.
- [7] CMS Collaboration. The CMS experiment at the CERN Large Hadron Collider. *JINST* **2008**, 3, S08004, doi:10.1088/1748-0221/3/08/S08004.
- [8] CMS Collaboration. The performance of the CMS muon detector in proton-proton collision at $\sqrt{s} = 7$ TeV at the LHC. *JINST* **2013**, 8, P11002, doi:10.1088/1748-0221/8/10/P11002.
- [9] MATLAB 8. The MathWorks Inc.: Natick, MA, USA.
- [10] Belau, E.; Klanner, R.; Lutz, G.; Neugebauer, E.; Seebrunner, H.J.; Wylie, A. Charge collection in silicon strip detector *Nucl. Instrum. and Method Phys. Res. A* **1983** 214 253-260.
- [11] Landi, G. Properties of the center of gravity as an algorithm for position measurements *Nucl. Instrum. and Methods Phys. Res. A* **2002** 485 698-719.
- [12] Landi, G.; Problems of position reconstruction in silicon microstrip detectors, doi 10.1016/j.nima.2005.08.094 *Nucl. Instr. and Methods Phys. Res. A* **2005** 554 226.
- [13] Landi, G.; Landi, G. E. "Asymmetries in Silicon Microstrip Response Function and Lorentz Angle" arXiv:1403.4273[physics.ins-det] <http://arxiv.org/abs/1403.4273>
- [14] Adriani, O.; Bongi, M.; Bonechi, L.; Bottai, S.; Castellini, G.; Fedele, D.; Grandi, M.; Landi, G.; Papini, P.; et al. "In-flight performance of the PAMELA magnetic spectrometer" 16th *International Workshop on Vertex Detectors* September 2007 NY. USA. PoS(Vertex 2007)048